Preclinical Characterization of G1T28: A Novel CDK4/6 Inhibitor for Reduction of Chemotherapy-Induced Myelosuppression

John E. Bisi[1], Jessica A. Sorrentino[1], Patrick J. Roberts[1], Francis X. Tavares[2], and Jay C. Strum[1]

Abstract

Chemotherapy-induced myelosuppression continues to represent the major dose-limiting toxicity of cytotoxic chemotherapy, which can be manifested as neutropenia, lymphopenia, anemia, and thrombocytopenia. As such, myelosuppression is the source of many of the adverse side effects of cancer treatment including infection, sepsis, bleeding, and fatigue, thus resulting in the need for hospitalizations, hematopoietic growth factor support, and transfusions (red blood cells and/or platelets). Moreover, clinical concerns raised by myelosuppression commonly lead to chemotherapy dose reductions, therefore limiting therapeutic dose intensity, and reducing the antitumor effectiveness of the treatment. Currently, the only course of treatment for myelosuppression is growth factor support which is suboptimal. These treatments are lineage specific, do not protect the bone marrow from the chemotherapy-inducing cytotoxic effects, and the safety and toxicity of each agent is extremely specific. Here, we describe the preclinical development of G1T28, a novel potent and selective CDK4/6 inhibitor that transiently and reversibly regulates the proliferation of murine and canine bone marrow hematopoietic stem and progenitor cells and provides multilineage protection from the hematologic toxicity of chemotherapy. Furthermore, G1T28 does not decrease the efficacy of cytotoxic chemotherapy on RB1-deficient tumors. G1T28 is currently in clinical development for the reduction of chemotherapy-induced myelosuppression in first- and second-line treatment of small-cell lung cancer. *Mol Cancer Ther; 15(5); 783–93. ©2016 AACR.*

Introduction

The cell cycle is a highly conserved and regulated process by which genomic integrity and replicative capacity must be maintained for proper cell maintenance and proliferation. The cell cycle consists of four distinct phases: G_1 or Gap1 phase where cells grow and synthesize proteins in preparation for DNA synthesis; S-phase, where DNA synthesis occurs; G_2 or Gap2 phase postsynthesis where cells continue to synthesize proteins to increase mass in preparation for mitosis; and finally, M-phase in which the DNA divides and the parent cell undergoes cytokinesis to produce two daughter cells (1). Regulation of this process is maintained by a series of highly conserved proteins referred to as cyclins, and their catalytic binding partners, cyclin-dependent kinases (CDK). The G_1 to S checkpoint is a critical restriction point in the process of cell division. Cells are maintained in a quiescent state until the proper signal is achieved for reentry into the cell cycle. Throughout G_1, expression of the D-type cyclins (D1, D2, D3) increases until active complexes with

CDK4/6 are formed. Active CDK4/6 complexes partially phosphorylate RB, which allows partial derepression of the transcription factor *E2F*. This induces additional transcript production including CCNE1. Cyclin E will bind CDK2 to form active complexes that results in the hyperphosphorylation of RB and drives the cells through late G_1 into S-phase. Inhibition of CDK4/6-cyclin D by the tumor suppressor CDKN2A leads to a G_1 arrest and cell-cycle progression is halted (2).

Inhibitors of cyclin-dependent kinases have been in clinical development for more than two decades (3). However, toxicity due to poor specificity has limited their therapeutic potential in oncology. More recently, potent and selective CDK4/6 inhibitors have received a significant level of attention with the report by Pfizer of robust progression-free survival data for postmenopausal women with estrogen receptor (ESR1) positive, ERBB2-negative metastatic breast cancer receiving the CDK4/6 inhibitor palbociclib in combination with letrozole, an aromatase inhibitor. This led to "Breakthrough Therapy" designation by the FDA and the subsequent approval of palbociclib in February 2015. Likewise, both Novartis and Eli Lilly and Company are advancing their proprietary CDK4/6 inhibitors into phase III clinical trials for hormone-responsive breast cancer as well as a variety of RB-dependent tumor types. Although targeted therapies have been shown to be effective in appropriately defined settings, the use of cytotoxic chemotherapies is still the cornerstone for treating a large number of patients. However, the most effective chemotherapies are limited in their utility due to myelosuppression. Chemotherapy-induced myelosuppression often results in dose reductions and treatment delays that adversely affect efficacy and produce serious adverse toxicities such as febrile neutropenia.

[1]G1 Therapeutics, Research Triangle Park, North Carolina. [2]ChemoGenics BioPharma, Research Triangle Park, North Carolina.

Corresponding Author: Jay C. Strum, G1 Therapeutics, 79 T.W. Alexander Drive, 4401 Research Commons, Suite 105, Research Triangle Park, NC 27709. Phone: 919-213-9835; Fax: 919-741-5830; E-mail: jcs@g1therapeutics.com

Bisi et al.

Table 1. Biochemical profiling of G1T28

	Selectivity							
	Cdk4/CycD1	Cdk6/CycD3	Cdk2/CycA	Cdk2/CycE	Cdk5/p25	Cdk5/p35	Cdk7/CycH/Mat1	Cdk9/CycT
Mean (µmol/L)	0.001	0.004	1.29	2.51	1.71	1.24	4.64	0.05
SEM	0.0002	0.001	0.10	0.25	0.48	0.04	0.39	0.01
n	9	3	6	6	3	3	3	3

Bone marrow hematopoietic stem and progenitor cells (HSPC) have been found to be highly dependent upon CDK4/6 for proliferation (ref. 4; and He et al., Pharmacological quiescence by CDK4/6 inhibition protects hematopoietic stem cells from chemotherapy induced proliferative exhaustion; submitted for publication). In addition, the transient arrest of these cells with a potent, selective CDK4/6 inhibitor has been shown to protect blood cell counts and prolong survival in mice exposed to chemotherapy or lethal doses of radiation (4, 5). Although many tumors are CDK4/6 dependent, more than 300,000 patients are diagnosed every year whose tumors are functionally CDK4/6 independent (3). These include small-cell lung cancer (SCLC; ref. 6), triple-negative breast cancer (7), bladder (8), human papilloma virus (HPV) associated head and neck (9), and prostate cancer (10, 11). The standard of care for many of these patients is myelosuppressive chemotherapy. The transient arrest of HSPCs by a CDK4/6 inhibitor during the administration of chemotherapy in these patients has the potential to protect the bone marrow and immune system from the cytotoxic effects of chemotherapy, while not adversely impacting the antitumor effects. This may translate to a decreased nadir and faster recovery of circulating blood cells, prevention of bone marrow exhaustion and the preservation of immune cell number and function, thereby allowing a more robust host immune response to the tumor.

G1T28 is a CDK4/6 inhibitor being developed to reduce chemotherapy-induced multilineage myelosuppression. This article describes the identification of G1T28 as a potent and selective CDK4/6 inhibitor that inhibits the phosphorylation of RB and induces an exclusive, reversible G_1 arrest. In vitro and in vivo, G1T28 protects RB competent cells from damage by chemotherapy as assessed by γH2AX and apoptosis through caspase-3/7 activation. In vivo, G1T28 regulates the proliferation of HSPCs in both mouse and canine bone marrow, in a reversible, dose- and time-dependent manner. Pretreatment of mice with G1T28 allows a faster recovery of complete blood counts (CBC) following chemotherapy. In addition, G1T28 does not protect RB-deficient tumors from chemotherapy but, instead, adds to the antitumor effect. G1T28 has recently been tested in a phase I, healthy volunteer pharmacokinetics and safety study (ref. 12; and Roberts et al., Phase 1A trial to evaluate safety and biologic activity in the bone marrow of G1T28, a CDK4/6 inhibitor; submitted for publication) and two phase Ib/IIa studies have been initiated in small-cell lung cancer to assess the potential for reduction of chemotherapy-induced multilineage myelosuppression (13, 14).

Materials and Methods

Chemical

G1T28 [2′-((5-(4-methylpiperazin-1-yl)pyridin-2-yl)amino)-7′,8′-dihydro-6′H-spiro[cyclohexane-1,9′-pyrazino[1′,2′:1,5]pyrrolo[2,3-d]pyrimidin]-6′-one] was synthesized and characterized for purity and identity as an HCl salt at ChemoGenics BioPharma, LLC in collaboration with G1 Therapeutics, Inc.

Nanosyn CDK in vitro assay

Compounds were tested in CDK2-CYCLIN A, CDK2-CYCLIN E, CDK4-CYCLIN D1, CDK6-CYCLIN D3, CDK5-p25, CDK5-p35, CDK7-CYCLIN H-MAT1, and CDK9-CYCLIN T kinase assays by Nanosyn, Inc. The assays were completed using microfluidic kinase detection technology (Caliper Assay Platform). The compounds were tested in 12-point dose–response format in singlicate at the Km for ATP. Phosphoacceptor substrate peptide concentration used was 1 µmol/L and staurosporine was used as the reference compound for all assays.

KINOMEscan primary screen and K_d determination

G1T28 was profiled at DiscoveRx using their KINOMEscan and scanMAX screening technology (15). Briefly, G1T28 was tested at 100 and 1,000 times the biochemical IC_{50} as described in Table 1. All target kinases that responded to greater than 90% inhibition were tested as individuals for K_d determination.

Cell lines

Cell lines were obtained from ATCC. HS68, A2058, WM2664, and MCF-7 cells were grown in DMEM (Life Technologies) containing 10% FBS (HyClone) and 1× Glutamax (Life Technologies). ZR-75-1, NCI-H69, and SHP77 cells were grown in RPMI1640 (CellGro) containing 10% FBS and 1× Glutamax. The SUP-T1 cells (Sigma-Aldrich) were grown in RPMI1640 containing 10% FBS and 1× Glutamax. Cell lines were authenticated using short tandem repeat analysis at ATCC.

Western blots

HS68, WM2664, and A2058 cells were treated with 300 nmol/L G1T28 or DMSO (0.1%), for 4, 8, 16, or 24 hours. Whole cell extracts were prepared using 1× radioimmunoprecipitation assay buffer (RIPA; Thermo Fisher Scientific) containing 1x HALT protease and phosphatase inhibitors (Thermo Fisher Scientific). Total protein concentration was determined by using the bicinchoninic acid (BCA) Protein Assay Kit (PIERCE), according to the manufacturer's instructions. Fifteen micrograms of protein was heat denatured for 10 minutes at 70°C and resolved by Novex NuPAGE SDS–PAGE gel system (Thermo Fisher Scientific) and transferred to 0.45 µm nitrocellulose membrane by electroblotting. Membranes were blocked in LiCor Membrane Blocking Buffer and incubated overnight with rabbit anti-pRb (Ser807/811) antibody (Cell Signaling Technology) at a 1:1,000 dilution and mouse anti-MAPK antibody (Cell Signaling Technology) at a 1:2,000 dilution, as a loading control. Secondary antibodies (LiCor) were Goat anti-rabbit (680RD) and Goat anti-mouse (800CW) at a 1:15,000 dilution. Blots were incubated for 1 hour, washed and imaged using LiCor ImageStudio software (Version 4.0.21).

For H69, MCF7, SupT1, and ZR75-1 Western blot analysis, protein was processed as described previously. Antibodies to total RB (Cell Signaling Technology) and β-tubulin (Cell Signaling Technology) run as a loading control were assessed. A goat anti-rabbit (680RD; LiCor) secondary antibody was utilized at a dilution of 1:15,000.

Cell-cycle analysis

HS68 cells were treated for 24 hours with G1T28 at 10, 30, 100, 300, 1,000, or 3,000 nmol/L final concentration. Cells were harvested and fixed in ice-cold methanol (Sigma-Aldrich). Fixed cells were stained with 20 μg propidium iodide (Sigma-Aldrich), 50 μg RNAse A (Sigma-Aldrich) in PBS-CMF (calcium magnesium free) + 1% BSA, Fraction V (Fisher Scientific). Samples were processed on Cyan ADP Analyzer (Beckman Coulter), and cell-cycle analysis was completed using FlowJo software (Version 10.0.8; Tree Star).

Cell proliferation

SupT1, MCF7, ZR-75-1, A2058, and H69 cells were seeded at 1,000 cells per well in Costar 3903 96-well plates. After 24 hours, plates were dosed with G1T28 at a nine-point dose concentration from 10 μmol/L to 1 nmol/L. Cell viability was determined after 4 or 6 days using the CellTiter-Glo assay (Promega) following the manufacturer's recommendations. Plates were processed on Bio-Tek Synergy2 multimode plate reader and data analyzed using GraphPad Prism 5 statistical software.

γH2AX and caspase-3/7 activation

For the γH2AX assay, 30,000 HS68 cells were plated per well in 12-well plates and incubated for 24 hours at 37°C. Cells were incubated with 10, 30, 100, 300, or 1,000 nmol/L G1T28 or dimethyl sulfoxide (Sigma-Aldrich) as vehicle control for 16 hours. Plates were subsequently dosed with chemotherapy [5 μmol/L etoposide (Selleckchem), 1 μmol/L doxorubicin (Bedford Laboratories), 100 μmol/L carboplatin (APP Pharmaceuticals, LLC), 156 nmol/L camptothecin (Sigma-Aldrich), or 250 nmol/L paclitaxel (Sigma-Aldrich)]. For γH2AX, cells were harvested for analysis 8 hours after exposure to chemotherapy. Cells were fixed and stained using the H2AX Phosphorylation Assay Kit (Millipore) by the manufacturer's instruction. γH2AX-positive HS68 cells were quantified using FACSCalibur Flow Cytometer (BD BioSciences) and FlowJo analysis software.

For the *in vitro* caspase-3/7 assays, HS68, H69, and SHP77 cells were seeded at 1,000 cells per well in Costar 3903 96-well plates. Cells were incubated with 10, 30, 100, 300, or 1,000 nmol/L G1T28 or dimethyl sulfoxide (Sigma-Aldrich) as vehicle control for 16 hours. Plates were subsequently dosed with chemotherapy as previously described and were analyzed directly in the plates 48 hours after chemotherapy treatment. Caspase-3/7 induction was measured using Caspase-Glo 3/7 Assay System (Promega) by following the manufacturer's recommended instructions.

In vitro washout experiments

Twenty-four hours after seeding on 60-mm dishes, HS68 cells were treated with G1T28 at a 300 nmol/L final concentration for 24 hours. Wells were washed twice with PBS-CMF, and then replenished with fresh culture medium. The cells were further incubated for a series of time points ($t = 16, 24, 40, 48$ hours after washout). At the conclusion of the experiment, cells were harvested, fixed, and stained for cell-cycle analysis as described previously.

Pharmacodynamic assessment of G1T28 in mouse bone marrow

Eight-week-old female FVB/N mice (Jackson Laboratory) were given a single oral dose of vehicle alone (20% Solutol, Sigma-Aldrich) or G1T28 at 50, 100, or 150 mg/kg, followed 11 or 23 hours later by a single intraperitoneal injection of 100 μg 5-ethynyl-2′-deoxyuridine (EdU, Life Technologies) as the Institutional Animal Care and Use Committee (IACUC) approved at University of North Carolina (Chapel Hill, NC). Mice were euthanized 1 hour after EdU injection (i.e., total G1T28 treatment of 12 or 24 hours), and Lineage-negative cells (Lin⁻) were isolated using biotin anti-mouse lineage panel (BioLegend) and anti-biotin microbeads (Miltenyi Biotec). Lin⁻ cells were stained for EdU following the manufacturer's instructions.

Peripheral blood analysis of 5-FU and G1T28 in mice

FVB/N female mice were given single oral doses of vehicle or G1T28 at 150 mg/kg, followed 30 minutes later by a single intraperitoneal dose of 5-fluorouracil (5-FU) at 150 mg/kg. CBCs were measured every 2 days starting on day 6. Data reported are from day 6 (Platelets), day 10 [white blood cells (WBC), neutrophils (Neu), lymphocytes (Lymph)], or day 16 [red blood cells (RBC)]. The IACUC committee at the University of North Carolina (Chapel Hill, NC) approved all protocols.

Caspase-3/7 activation in murine bone marrow

C57Bl/6 female mice were given single oral doses of vehicle, 50 mg/kg or 100 mg/kg of G1T28 followed 30 minutes later by a single intraperitoneal dose of etoposide at 2 mg/kg. Six hours after treatment, mice were euthanized and bone marrow harvested. Caspase-3/7 activation was assessed using 100,000 bone marrow cells per well as previously described. The IACUC committee at Charles River Laboratories approved all protocols.

G1T28 and topotecan efficacy in RB-deficient tumors

Female athymic nude mice were implanted with H69 cells and monitored until treatment initiation. Once tumors reached an acceptable size (150 mm³), mice were dosed in various combinations of G1T28 and topotecan for 5 days per week for 4 weeks. Tumors were measured for up to 60 days after treatment. All mice that reached excessive tumor burden before 60 days were humanely euthanized. All protocols were IACUC approved and experiments were completed at South Texas Accelerated Research Treatments (START). Topotecan and G1T28 levels in blood plasma from the mice treated with G1T28 and/or topotecan were processed and analyzed using established methods at Bioanalytical Systems, Inc.

Results

Identification of G1T28

Rational structure–based drug design was utilized to create a novel, proprietary Tricyclic Lactam scaffold with activity against cyclin-dependent kinases. Multiple rounds of structure activity relationship studies were conducted to optimize the potency, selectivity, and cellular properties of this scaffold. To assess potency, biochemical profiling was completed against CDK4/cyclin D1 and CDK6/cyclin D3. To maximize selectivity, compounds were profiled against CDK2/cyclin A and CDK2/cyclin E. Compounds with 100-fold or greater selectivity for CDK4/cyclin D1 versus CDK2/cyclin E were profiled in cell-based screens to look for G_1 arrest in normal HS68 fibroblast cells, with a functioning RB pathway. Compounds with cellular EC_{50}s < 100 nmol/L and an exclusive G_1 arrest profile through 1 μmol/L, were further investigated for inhibition of RB phosphorylation, caspase-3/7 activation, and γH2AX induction. On

the basis of physicochemical, absorption, distribution, metabolism and excretion and pharmacokinetic properties, candidate compounds were tested in vivo for pharmacodynamic activity (G_1 arrest of HSPCs). G1T28, [2′-((5-(4-methylpiperazin-1-yl) pyridin-2-yl)amino)-7′,8′-dihydro-6′H-spiro[cyclohexane-1,9′-pyrazino[1′,2′:1,5]pyrrolo[2,3-d]pyrimidin]-6′-one], was selected as the lead candidate small-molecule reversible kinase inhibitor which potently and selectively targets both CDK4/cyclin D1 and CDK6/cyclin D3 and has optimal in vivo biologic activity as an ideal chemoprotectant (Fig. 1A). All preclinical characterization was completed with the dihydrochloride salt form.

In microfluidic kinase detection technology (Caliper Assay Platform) assays (Nanosyn, Inc.), G1T28 reversibly inhibited CDK4/cyclin D1 and CDK6/cyclin D3 with an IC_{50} of 1 nmol/L and 4 nmol/L, respectively. This activity was highly selective versus other CDK/cyclin complex family members (Table 1). In particular, inhibition of CDK2/cyclin A, CDK2/cyclin E, CDK5/p25, CDK5/p35, and CDK7/cyclin H/Mat1 was more than 3 orders of magnitude less than CDK4/cyclin D1 and CDK9/cyclin T was approximately 50-fold less than CDK4/cyclin D1. Kinase selectivity was further interrogated in a screen of 468 protein kinases (KINOMEscan, DiscoveRx) at 100 nmol/L and 1 μmol/L (data not shown) concentrations. Profiling at 100 times the IC_{50} showed high degree of selectivity using an S-Score of 35 (Fig. 1B, right), with significant selectivity at an S-Score of 1 (Fig. 1B, left). Those protein kinases with greater than 90% inhibition were followed up for K_d determination (Supplementary Table S1). Additional kinases of interest involved in cell growth and proliferation were tested including AKT1, Aurora B, Erk1, and Wee1 with no appreciable activity observed.

G1T28 reversibly pauses the cell cycle in the G_1 phase in only CDK4/6-dependent cell lines

The cellular potency of G1T28 in producing a G_1 cell-cycle arrest was tested in CDK4/6-dependent (HS68, WM2664) and CDK4/6-independent (A2058) cell lines. G1T28 only inhibited the CDK4/6-dependent cells, with an EC_{50} of 30 nmol/L in HS68 cells (Fig. 1C). In the CDK4/6-independent A2058 cell line, there was no decrease in S-phase with G1T28 treatment (brown arrow, Fig. 1C, left). However, in both the HS68 and WM2664 cell lines, there was a significant dose-dependent decrease in S-phase with a concomitant increase in G_1. In HS68 cells, up to 98% of cells were in G_1 after 24 hours of treatment of either 300 nmol/L or 1 μmol/L (Fig. 1C, right). This G_1 arrest was maintained through 3 μmol/L demonstrating that G1T28 elicited a clean G_1 arrest for >3,000 times the enzymatic IC_{50}.

In normal cycling cells, the CDK4/6-cyclin D complex phosphorylates RB as an immediate downstream effect. Once phosphorylated, RB dissociates from cell-cycle promoting transcription factors, which then drive G_1–S-phase transition (16). Conversely, inhibition of RB phosphorylation leads to G_1 cell-cycle arrest. Therefore, the CDK4/6 specificity of G1T28 was confirmed by phospho-RB Western blot analysis. After incubation with HS68, WM2664, or A2058, G1T28 blocked RB phosphorylation in the RB-dependent cell lines by 16 hours after exposure, whereas the CDK4/6-independent cell line (A2058) exhibited no RB or pRB expression, as expected (Fig. 1D). This observation was confirmed by comparing additional RB competent and RB-deficient cell lines. As shown in Supplementary Fig. S1, RB competent cell lines were sensitive to growth inhibition when incubated with G1T28 whereas RB-deficient cell lines were resistant to growth inhibition.

To demonstrate the G1T28-induced G_1 cell-cycle arrest is transient and reversible, HS68 cells were treated with G1T28 at 300 nmol/L for 24 hours and cell-cycle analysis was completed at various times after treatment (0, 16, 24, 40, 48 hours). As previously seen, incubation with G1T28 for 24 hours induced a robust G_1 cell-cycle arrest (Fig. 1E, time = 0). By 16 hours after G1T28 washout, cells had reentered the cell cycle and demonstrated cell-cycle kinetics similar to untreated control cells (Fig. 1E). These results demonstrate that G1T28 causes a transient, and reversible G_1 arrest.

G1T28 protects CDK4/6-dependent cells from chemotherapy-induced damage in vitro

To demonstrate G1T28-induced G_1 arrest decreases chemotherapy-induced damage (i.e., apoptosis or DNA damage), HS68 cells (a surrogate model to represent CDK4/6-dependent HSPCs), were treated with G1T28 and an array of chemotherapies with differing mechanisms of action. Specifically, HS68 cells were pretreated with G1T28 or vehicle control for 16 hours, at which time indicated chemotherapies were added to the cultures. Cells were harvested 8 hours after treatment to measure γH2AX foci (DNA damage) and 48 hours after treatment to measure caspase-3/7 activity (apoptosis). Pretreatment of G1T28 in all DNA damaging chemotherapies tested (carboplatin, doxorubicin, etoposide, camptothecin) demonstrated a dose-dependent decrease in γH2AX foci suggesting an attenuation of chemotherapy-induced DNA damage (Fig. 2A). In addition, treatment of HS68 cells with G1T28 prior to chemotherapy treatment (DNA damaging agents previously described, as well as a DNA intercalator; 5-FU and an antimitotic; paclitaxel) elicited a robust dose-dependent decrease in caspase-3/7 activation suggesting an attenuation of apoptosis (Fig. 2B). The data show that a transient G1T28-mediated G_1 cell-cycle arrest in CDK4/6-sensitive cells decreases the in vitro toxicity of a variety of commonly used cytotoxic chemotherapy agents associated with myelosuppression.

G1T28 induces a reversible cell-cycle arrest in murine and canine HSPCs

To understand the temporal effect of G1T28 treatment on HSPC proliferation, the kinetics of G1T28-induced G_1 cell-cycle arrest and reversal in HSPCs were measured in young adult FVB/N female mice after a single oral gavage of G1T28 at 50, 100, or 150 mg/kg. G1T28 treatment resulted in a robust and dose-dependent suppression of proliferation in HSPCs at 12 hours, with EdU incorporation returning near baseline levels in a dose-dependent manner by 24 hours after administration (Fig. 3A). The data demonstrate that a single oral dose of G1T28 can produce reversible cell-cycle arrest in HSPCs in a dose-dependent manner in vivo.

To confirm the findings seen in murine bone marrow, the effect of G1T28 on dog bone marrow EdU incorporation was evaluated. Detailed methods can be found in the supplementary methods. In summary, dogs were given single 30-minute intravenous infusions of G1T28 at 0, 1, 5, and 15 mg/kg. Bone marrow was taken from the dogs at 8, 16, and 24 hours after infusion. Blood samples were taken from dogs at predose and 24, 48, 72, 168, 240, and 336 hours after the G1T28 dose to measure the plasma concentration of the drug. A dose-dependent decrease in bone marrow proliferation was observed, with higher dose levels producing a decrease in whole bone marrow proliferation similar to the decrease observed in mice (Supplementary Fig. S2B).
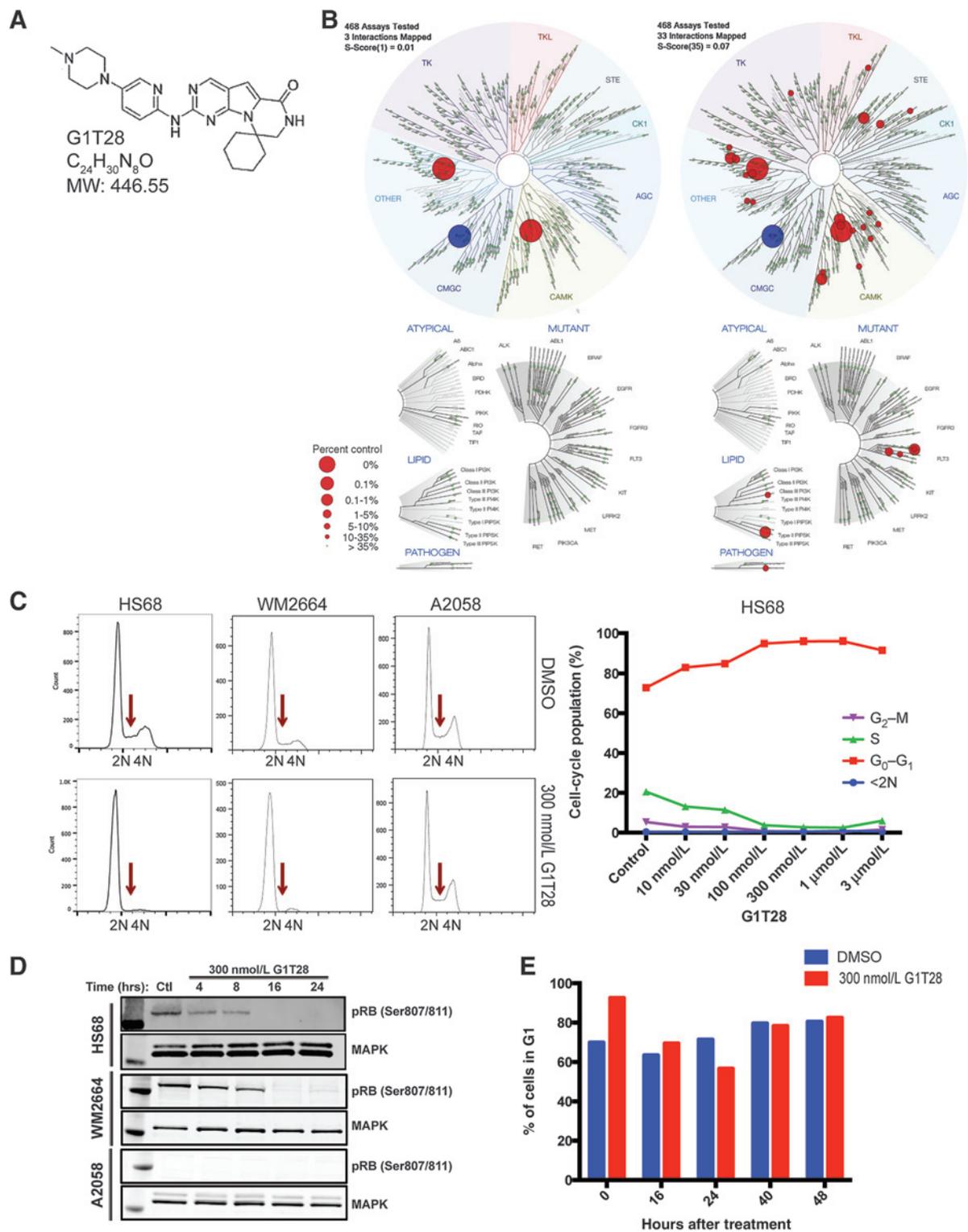
Figure 1.
Chemical structure, kinome specificity, and biochemical properties of G1T28. A, structure, molecular formula, and formula weight (free base and HCl salt) of G1T28. B, kinome binding specificity of G1T28 was measured by site-directed competition-binding assays (S-score = 1, left, S-score = 35, right). C, G1T28 reversibly inhibited the cell cycle in only CDK4/6-dependent cell lines (HS68 and WM2664). D, Western blot analysis demonstrating a time course of G1T28-dependent inhibition of RB phosphorylation at Serine 807/ 811. E, the CDK4/6-dependent cell line (HS68) was treated with 300 nmol/L G1T28 for 24 hours and cells were harvested at the indicated times following washout of G1T28 with media demonstrating the reversibility of G1T28. The percentage of cells in the G_1 phase is shown.

Bisi et al.
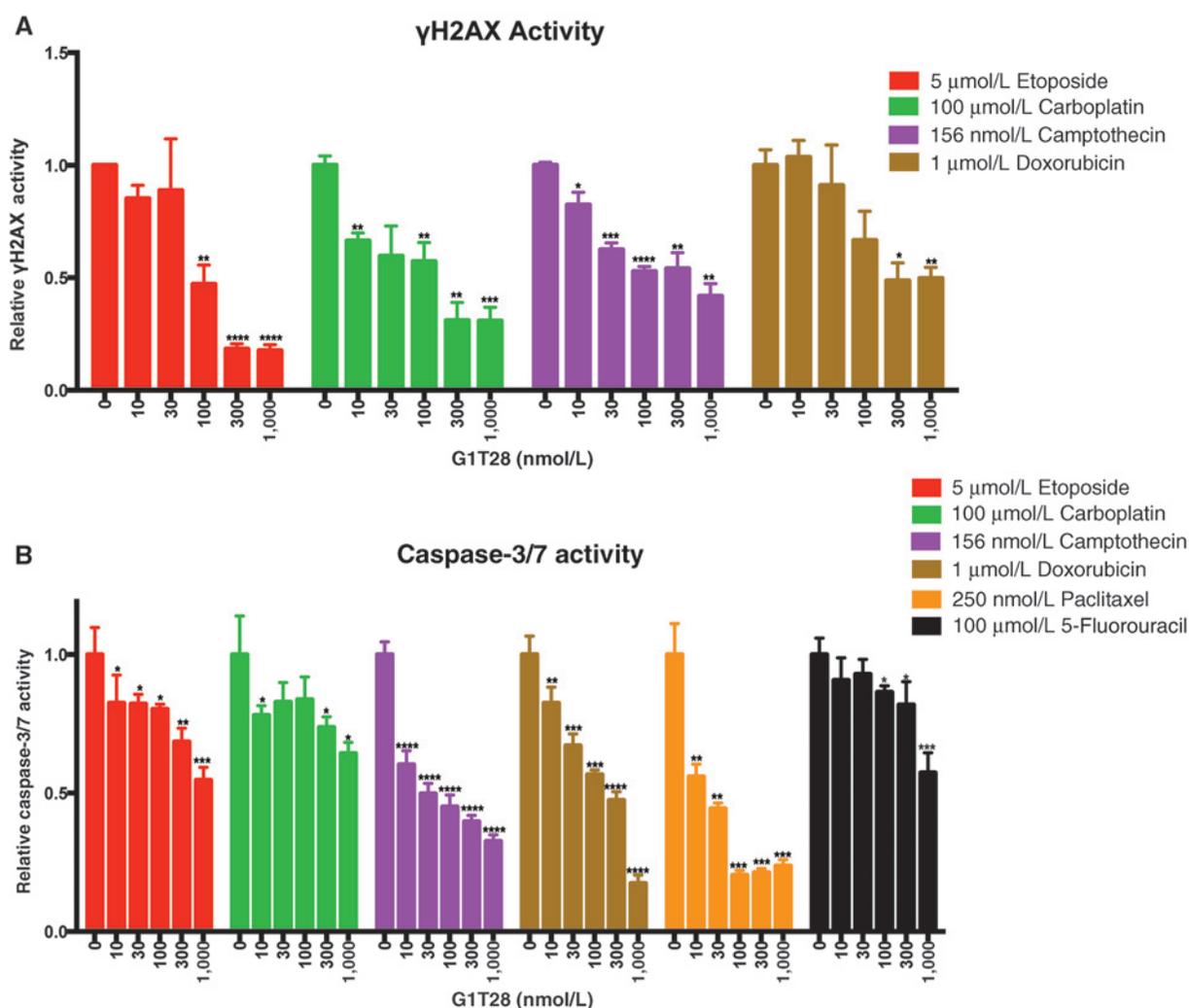
Figure 2.
G1T28 protects CDK4/6-dependent cells from chemotherapy-induced DNA damage and apoptosis *in vitro*. HS68 cells were incubated with G1T28 at the indicated doses for 16 hours followed by exposure to the indicated chemotherapy agents for 8 hours (γH2AX) or 48 hours (caspase 3/7) prior to harvest. A, direct DNA damage was measured through γH2AX flow cytometry staining. B, apoptosis was measured through caspase-3/7 activation in HS68 cells. *, $P \leq 0.05$; **, $P \leq 0.01$; ***, $P \leq 0.001$; ****, $P \leq 0.0001$. Error bars, SEM.

The biologic effect of the inhibition of bone marrow proliferation in both species was longer than the approximately 4-hour pharmacokinetic half-life of G1T28 in dogs and 5 hours in mice (Supplementary Fig. S2A, data not shown). This suggests that factors other than drug concentration, such as cell cycling times of various progenitors, will impact the duration of HSPC G_1 arrest. Finally, despite a robust G_1 arrest of the bone marrow that persisted for up to 24 hours at a dose of 15 mg/kg G1T28, only subtle changes were noted in CBCs (Supplementary Fig. S2C and S2D). This is further evidence that the G1T28-induced G_1 arrest is transient and reversible *in vivo*.

G1T28 protects mouse bone marrow cells from chemotherapy-induced apoptosis and attenuates chemotherapy-induced myelosuppression *in vivo*

To directly measure the effect of transient G_1 cell-cycle arrest of the HSPCs on chemotherapy-induced bone marrow toxicity, we determined the ability of G1T28 to prevent etoposide-induced

apoptosis of bone marrow cells in C57Bl/6 mice. Mice received vehicle or G1T28 30 minutes by oral gavage prior to etoposide, and bone marrow was harvested 6 hours after etoposide treatment. Caspase-3/7 activation increased 3-fold in bone marrow from mice that received etoposide (Fig. 3B), whereas mice that received G1T28 prior to etoposide showed a dose-dependent decrease in caspase-3/7 activation (Fig. 3B). In fact, mice given 100 mg/kg G1T28 30 minutes prior to etoposide treatment, exhibited only background levels of caspase-3/7 activity. These data demonstrate that G1T28 can protect the bone marrow from chemotherapy-induced apoptosis *in vivo*.

To expand upon these findings, the ability of G1T28 to attenuate chemotherapy-induced myelosuppression was evaluated using a well-characterized single-dose 5-FU regimen that is highly myelosuppressive in mice. FVB/N female mice were given single oral doses of vehicle or 150 mg/kg of G1T28, followed 30 minutes later by a single intraperitoneal dose of 150 mg/kg of 5-FU. Administration of G1T28 prior to 5-FU produced a faster recovery of all
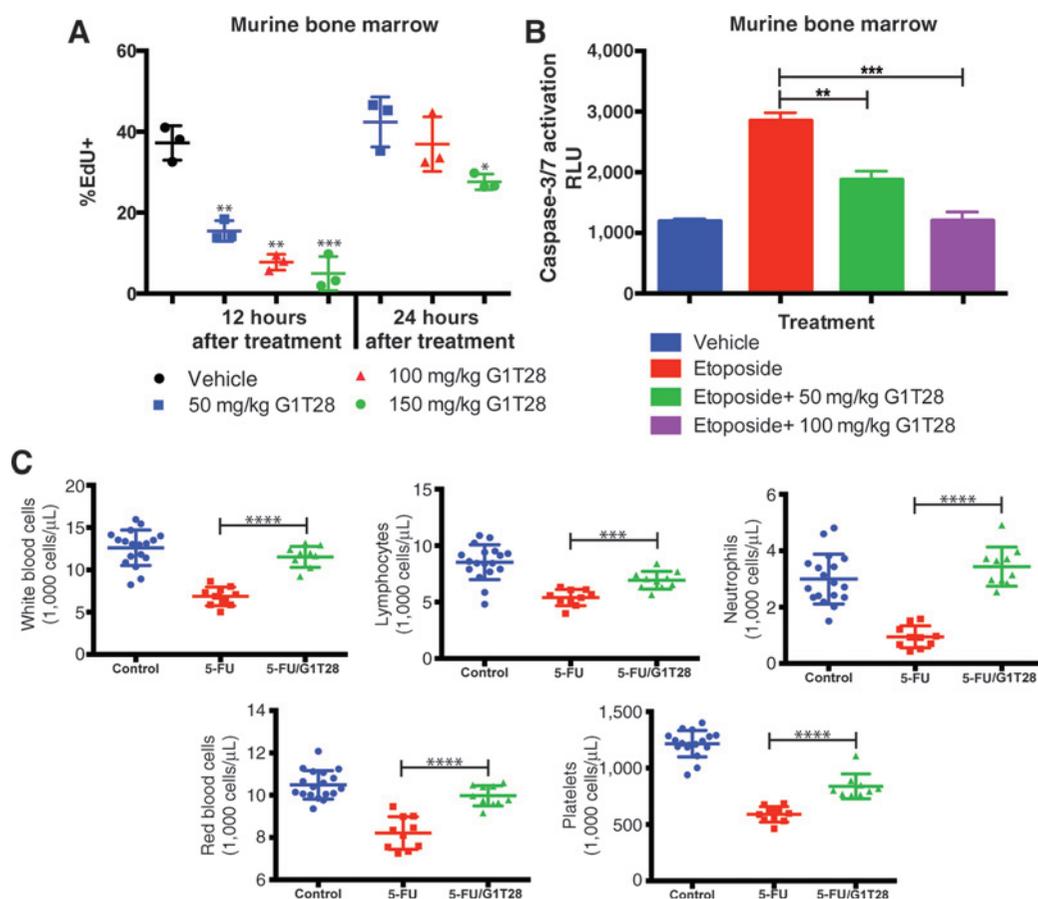
Figure 3.

G1T28 inhibits cellular proliferation in bone marrow leading to chemoprotection *in vivo*. A, FVB/N mice received a single dose of 50, 100, or 150 mg/kg G1T28 by oral gavage, and were pulsed with 100 µg of EdU 1 hour before harvest. Bone marrow was harvested at either 12 or 24 hours after G1T28 administration and lineage-negative cells (Lin⁻) were isolated. Data show relative proliferation of Lin⁻ cells at the indicated times following G1T28 administration. B, caspase activation in mouse bone marrow after etoposide treatment. Mice were given either 3 mg/kg etoposide only, or etoposide and G1T28 (50 or 100 mg/kg) 30 minutes prior to etoposide. Bone marrow harvested 6 hours after treatment shows a decrease in caspase-3/7 activation with G1T28 treatment. C, FBV/N mice were treated with G1T28 150 mg/kg or vehicle control by oral gavage 30 minutes prior to administration of 5-FU 150 mg/kg by intraperitoneal injection. CBCs were measured every 2 days starting on day 6. Data reported are from day 6 (Platelets), day 10 (WBC, Neu, Lymph), or day 16 (RBC). CBC analysis showed mice treated with 150 mg/kg 5-FU and 100 mg/kg G1T28 (30 minutes prior to 5-FU) show a faster recovery in all peripheral blood lineages. **, $P \leq 0.01$; ***, $P \leq 0.001$; ****, $P \leq 0.0001$. Error bars, SEM.

hematopoietic lineages from 5-FU-induced myelosuppression (Fig. 3C). The data demonstrate that treatment with G1T28 prior to 5-FU likely decreases 5-FU-induced damage by chemotherapy in HSPCs, thus accelerating blood count recovery after chemotherapy.

### RB-deficient cell lines are resistant to CDK4/6 inhibition

To use G1T28 to selectively protect the HSPC, while not antagonizing the intended antitumor activity of the chemotherapy, the tumor must be CDK4/6 independent. As RB is the direct downstream effector of CDK4/6, loss of RB is one marker of CDK4/6 independence. Previous findings have shown that RB-deficient cells are resistant to CDK4/6 inhibition (17–19). To demonstrate this finding with G1T28, a panel of RB-null SCLC cell lines was treated with DMSO or G1T28 for 24 hours. All SCLC cell lines (H69, H82, H209, H345, SHP-77) were confirmed to be RB null by Western blot analysis (Fig. 4A). The effect of CDK4/6 inhibition on proliferation was measured by flow cytometry using propidium iodide (PI) staining. All SCLC cell lines were resistant to CDK4/6 inhibition, with no change in the percent of cells in the

G_1-phase upon treatment (data from two representative cell lines are shown in Fig. 4B). These data are consistent with the previous findings that RB-deficient cells are resistant to CDK4/6 inhibition (4, 5, 20–23).

Coadministration of G1T28 does not antagonize the intended chemotherapy-induced cytotoxicity of SCLC cells *in vitro* or *in vivo*

To expand upon these findings and show that G1T28 does not antagonize the intended cytotoxicity of chemotherapy, the effect of coadministration of G1T28 with chemotherapy (cisplatin and etoposide) was evaluated in a panel of RB-null SCLC cell lines. As shown in data from two representative cell lines in Fig. 4C, coadministration of G1T28 across a dose range of 10 nmol/L to 1 µmol/L had no impact on the cytotoxicity of cisplatin (5 µmol/L) or etoposide (2.5 µmol/L). These findings are consistent with previous results that RB-deficient cells are intrinsically resistant to CDK4/6 inhibition and thus are not protected from the intended cytotoxicity of chemotherapy.
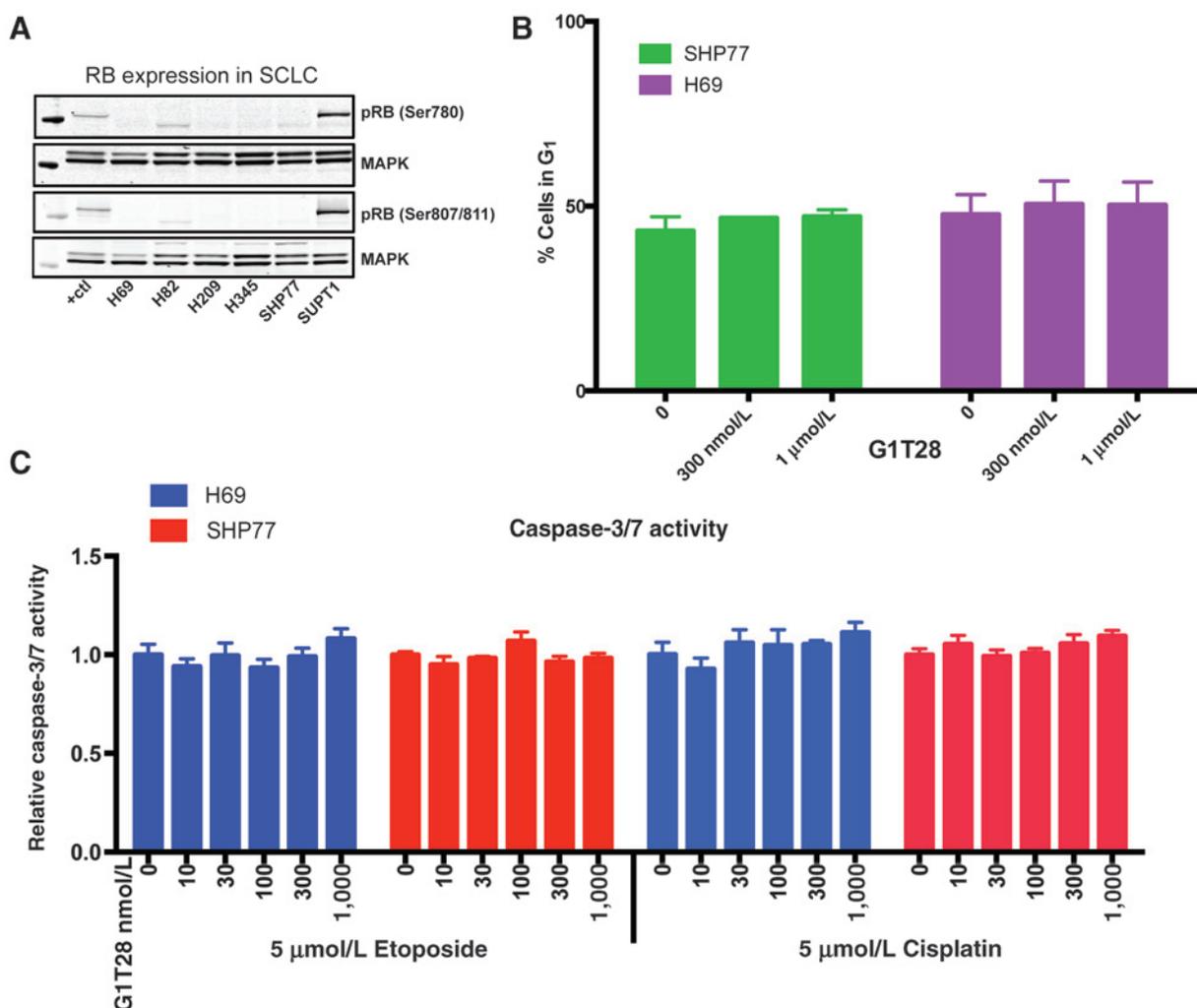
Figure 4.
Cells that are CDK4/6 independent are RB null and G1T28 does not cause protection from chemotherapy treatment. A, Western blot analysis of SCLC cell lines (H69, H82, H209, H345, Shp77) demonstrates these cells are RB null, whereas known CDK4/6-dependent cells (HS68 and SupT1) express RB. B, two representative CDK4/6-independent cell lines (SHP77 and H69) were treated with G1T28 or DMSO for 24 hours. Cell-cycle analysis was evaluated by propidium iodide incorporation and flow cytometry and demonstrated that the proportion of cells in the G_1 phase does not change with G1T28 exposure. C, CDK4/6-independent H69 and SHP77 SCLC cell lines were treated with the indicated doses of G1T28 or DMSO and either cisplatin or etoposide. Caspase-3/7 activity was measured and demonstrated no change with G1T28 exposure. All samples were normalized to the DMSO + DMSO treatment. Error bars, SEM.

To translate these findings *in vivo*, G1T28 was tested alone and in combination with topotecan in a SCLC xenograft model (H69) in athymic mice. H69 tumor bearing mice were treated with 100 mg/kg G1T28, 0.6 mg/kg topotecan, or 10, 50, or 100 mg/kg G1T28 30 minutes before topotecan. As expected, H69 tumors were resistant to single agent G1T28, as the cells are RB-null. Although single agent topotecan produced a robust tumor regression of the H69 tumors, the combination of G1T28 at 10, 50, or 100 mg/kg with topotecan was superior. During and after dosing, G1T28 potentiated the statistically significant ($P < 0.05$) effect of topotecan through study completion (Fig. 5A). Overall, G1T28 was well tolerated and did not antagonize the effects of chemotherapy. In fact, G1T28 potentiated the antitumor effect of topotecan in the H69 model, which could not be explained by a potential drug–drug interaction as the plasma levels of G1T28 and

topotecan were not affected by cotreatment (Supplementary Fig. S3). Potential mechanisms for this enhancement of chemotherapy efficacy effect are currently being explored.

Discussion

Each year in the United States, there are an estimated 300,000 new cases of cancer whose proliferation is controlled through a CDK4/6-independent pathway (3, 24). Of these, approximately 33,000 are cases of SCLC, 95% of which are attributed to tobacco exposure (25, 26). SCLC represents approximately 20% of all lung cancer cases and is the most aggressive and lethal lung cancer subtype (3). It is characterized by rapid tumor growth, early metastatic spread, and initial chemotherapy responsiveness followed by disease progression with resistant disease. Despite
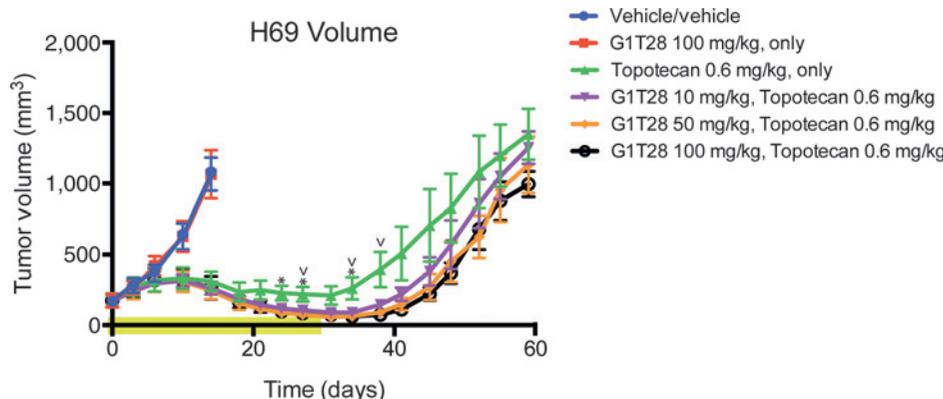
Figure 5.
G1T28 does not protect the effect of chemotherapy on CDK4/6-independent, RB-null SCLC *in vivo*. H69 SCLC cells were implanted into immune-deficient mice and the study initiated at a mean tumor volume of approximately 150 to 250 mm^3. G1T28 administered alone or 30 minutes before topotecan was well tolerated with no additive weight loss or toxicity. G1T28 was dosed at 10, 50, or 100 mg/kg/dose. Topotecan 0.6 mg/kg/dose was administered by intraperitoneal injection daily for 5 days of each week for 4 consecutive weeks. G1T28 does not decrease the efficacy of topotecan in the RB-null H69 SCLC cell line. *, $P \leq 0.05$, topotecan only compared with 50 mg/kg G1T28+Topotecan. $^\vee$, $P \leq 0.05$, topotecan only compared with 100 mg/kg G1T28+Topotecan. Error bars, SEM. Yellow bar, duration of dosing.

response rates of 70% to 85%, over 95% of patients with SCLC will die within 5 years of diagnosis. Myelosuppressive chemotherapy (e.g., platinum/etoposide for first line and topotecan as second line) is a cornerstone of SCLC treatment, however chemotherapy treatments in these patients are often poorly tolerated leading to dose reductions and treatment delays that minimize durable responses and decrease long-term survival (27). Although growth factors such as G-CSF have increased medical oncologists' ability to deliver myelotoxic therapies in patients with SCLC, neutropenia, anemia, and thrombocytopenia are still limiting toxicities of SCLC regimens. Considerable improvement in patient outcomes could be realized by maximizing the current treatment regimens through minimizing hematologic toxicity.

The RB tumor suppressor is a major negative cell-cycle regulator that is inactivated in approximately 11% of all human cancers, and nearly 100% of SCLC (24, 28). Moreover, activated CDK4/6 promotes G$_1$–S traversal by phosphorylating and inactivating RB. Importantly, cancers that inactivate RB do not require CDK4/6 activity for cell-cycle progression (17–19). As inactivation of RB is an obligate event in SCLC development (6), this tumor type is highly resistant to CDK4/6 inhibitors and coadministration of CDK4/6 inhibitors with cytotoxic chemotherapeutic agents such as those used in SCLC should not antagonize the efficacy of such agents. Furthermore, CDK4 has also been shown to phosphorylate SMAD3 thus inhibiting TGFβ-associated cell-cycle progression in Rb inactivated tumors (e.g., SCLC) suggesting G1T28 treatment could arrest Rb null cells resulting in protection of the tumor from chemotherapy (29, 30). However, the *in vitro* and *in vivo* data presented herein shows (i) G1T28 does not cause a cell-cycle arrest in Rb null cells (Fig. 1) and (ii) G1T28 does not protect Rb null tumor cells from chemotherapy-induced damage (Fig. 4) demonstrating G1T28 is not inhibiting the TGFβ-associated cell-cycle progression and any associated chemoprotection. In fact, G1T28/topotecan treatment of SCLC *in vivo* shows an increase in tumor efficacy when compared with topotecan alone demonstrating that G1T28 does not protect Rb incompetent SCLC from chemotherapy treatment (Fig. 5).

Previous reports have shown that bone marrow cells are dependent upon CDK4/6 for proliferation (4, 5). To take advantage of this biology and preserve bone marrow and immune system function during chemotherapy administration for patients whose tumors are CDK4/6 independent, the ideal compound should have the following properties. First, it should demonstrate high potency and selectivity for CDK4/6 compared with CDK2/cyclin E and CDK2/cyclin A. The active sites of CDK2 and CDK4/6 share significant homology. Until recently, it has proven very difficult to develop highly selective CDK4/6 inhibitors. Inhibiting CDK2/cyclin A would produce an S-phase arrest in cells rather than a clean G$_1$ arrest. Prolonged S-phase arrest could be cytotoxic in of itself, for example, the gastrointestinal toxicity seen with less selective CDK inhibitors, and could add to the cytotoxicity of chemotherapy. Second, an intravenously administered compound with a relatively short half-life could be beneficial so that the extent and duration of HSPC arrest can be tightly controlled, that is, G$_1$ arrest of HSPCs during and for several chemotherapy half-lives after the last chemotherapy dose, followed by rapid reentry of HSPCs into the cell cycle. The pharmacokinetic variability of orally delivered compounds that possess long half-lives and accumulate on repeat dosing would arrest the bone marrow far too long and contribute to myelosuppression of the cytotoxic chemotherapies. Finally, the compound should demonstrate favorable physiochemical properties. Considering the Lipinski rule of five, the compound should have a molecular weight of less than 500, not more than five hydrogen bond donors, a LogP of less than 5, and fewer than 10 hydrogen bond acceptors (31).

The work described herein provides support for G1T28 having ideal properties to be used as an agent to preserve bone marrow and immune system function during chemotherapy. It is a highly potent and selective CDK4/6 inhibitor that is biologically active when delivered intravenously or orally. Assessment of kinase inhibition *in vitro* has been utilized successfully for many years to identify putative biologic activities of small-molecule inhibitors. These results must, however, be placed in context with the cellular and *in vivo* results observed. Albeit G1T28 appeared to

potently bind additional kinases (Supplementary Table S1) we did not observe the expected biologic result of inhibition of these kinases. For example, we did not observed any increase in cell death or apoptosis as measured by cell-cycle analysis (Fig. 1C) or γH2AX induction (Fig. 2A) which could result from inhibiting kinases such as GAK, MEK5, PRKD2, and PRKD3. We continue to assess the potential for off-target activity as well as complementary activity by other targets that G1T28 may bind.

In additon, G1T28 inhibits the phosphorylation of RB and induces an exclusive, reversible G_1 arrest. *In vitro* and *in vivo*, G1T28 protects cells from damage by chemotherapy as assessed by γH2AX and caspase-3/7 activation. *In vivo*, G1T28 reversibly and in a dose-dependent manner, regulates the proliferation of HSPCs. Pretreatment of mice with oral G1T28 allows for the faster recovery of CBCs following chemotherapy treatment. Likewise, oral G1T28 does not protect RB-deficient tumors from chemotherapy but adds to the antitumor effect. Although this effect was found in athymic mice that lack T lymphocytes, it is still possible that the enhanced efficacy is due to preservation of other immune cell types such as natural killer cells. Although G1T28 protects immune cell numbers through its effect on the bone marrow, the effect of G1T28 on immune cell function is currently unknown but is an area of active research.

G1T28 has recently been tested in a phase I, healthy volunteer pharmacokinetics and safety study (NCT02243150; Roberts et al., Phase 1A trial to evaluate safety and biologic activity in the bone marrow of G1T28, a CDK4/6 inhibitor; submitted for publication) and two phase Ib/IIa studies in small cell lung cancer (NCT02499770 and NCT02514447) have been initiated. The proof of concept studies will provide data on the ability of G1T28 to reduce chemotherapy-induced myelosuppression and improve patient outcomes.

Authors' Contributions

Conception and design: J.E. Bisi, J.A. Sorrentino, P.J. Roberts, J.C. Strum
Development of methodology: J.E. Bisi, J.A. Sorrentino, P.J. Roberts
Acquisition of data (provided animals, acquired and managed patients, provided facilities, etc.): J.E. Bisi, J.A. Sorrentino, P.J. Roberts
Analysis and interpretation of data (e.g., statistical analysis, biostatistics, computational analysis): J.E. Bisi, J.A. Sorrentino, P.J. Roberts
Writing, review, and/or revision of the manuscript: J.E. Bisi, J.A. Sorrentino, P.J. Roberts, J.C. Strum
Administrative, technical, or material support (i.e., reporting or organizing data, constructing databases): J.E. Bisi, J.A. Sorrentino, P.J. Roberts
Study supervision: J.E. Bisi, J.A. Sorrentino, P.J. Roberts, J.C. Strum
Other (designed and synthesized G1T28 and related selective CDK 4/6 compounds as a founder/employee of ChemoGenics BioPharma on a collaborative basis for G1 Therapeutics): F.X. Tavares

References

1. Sherr CJ. Mammalian G1 cyclins and cell cycle progression. Proc Assoc Am Physicians 1995;107:181–6.
2. Donjerkovic D, Scott DW. Regulation of the G1 phase of the mammalian cell cycle. Cell Res 2000;10:1–16.
3. Asghar U, Witkiewicz AK, Turner NC, Knudsen ES. The history and future of targeting cyclin-dependent kinases in cancer therapy. Nat Rev Drug Discov 2015;14:130–46.
4. Johnson SM, Torrice CD, Bell JF, Monahan KB, Jiang Q, Wang Y, et al. Mitigation of hematologic radiation toxicity in mice through pharmacological quiescence induced by CDK4/6 inhibition. J Clin Invest 2010;120:2528–36.
5. Roberts PJ, Bisi JE, Strum JC, Combest AJ, Darr DB, Usary JE, et al. Multiple roles of cyclin-dependent kinase 4/6 inhibitors in cancer therapy. J Natl Cancer Inst 2012;104:476–87.
6. George J, Lim JS, Jang SJ, Cun Y, Ozretic L, Kong G, et al. Comprehensive genomic profiles of small cell lung cancer. Nature 2015;524:47–53.
7. Perou CM. Molecular stratification of triple-negative breast cancers. Oncologist 2011;16Suppl 1:61–70.
8. Damrauer JS, Hoadley KA, Chism DD, Fan C, Tiganelli CJ, Wobker SE, et al. Intrinsic subtypes of high-grade bladder cancer reflect the hallmarks of breast cancer biology. Proc Natl Acad Sci U S A 2014;111:3110–5.
9. Munger K, Jones DL. Human papillomavirus carcinogenesis: an identity crisis in the retinoblastoma tumor suppressor pathway. J Virol 2015;89:4708–11.
10. Macleod KF. The RB tumor suppressor: a gatekeeper to hormone independence in prostate cancer? J Clin Invest 2010;120:4179–82.
11. Sharma A, Yeow WS, Ertel A, Coleman I, Clegg N, Thangavel C, et al. The retinoblastoma tumor suppressor controls androgen signaling and human prostate cancer progression. J Clin Invest 2010;120:4478–92.
12. G1 Therapeutics I. Safety, Pharmacokinetic and pharmacodynamic study of the CDK 4/6 inhibitor G1T28-1. Available from: https://ClinicalTrials.gov/show/NCT02243150
13. G1 Therapeutics I. G1T28 (CDK 4/6 Inhibitor) in Combination With Etoposide and Carboplatin in Extensive Stage Small Cell Lung Cancer (SCLC). Available from: https://ClinicalTrials.gov/show/NCT02499770
14. G1 Therapeutics I. Study of G1T28 in Patients With Previously Treated Extensive Stage SCLC Receiving Topotecan Chemotherapy. Available from: https://ClinicalTrials.gov/show/NCT02514447
15. Fabian MA, Biggs WH3rd, Treiber DK, Atteridge CE, Azimioara MD, Benedetti MG, et al. A small molecule-kinase interaction map for clinical kinase inhibitors. Nat Biotechnol 2005;23:329–36.
16. Nevins JR. The Rb/E2F pathway and cancer. Hum Mol Genet 2001;10:699–703.
17. Toogood PL, Harvey PJ, Repine JT, Sheehan DJ, VanderWel SN, Zhou H, et al. Discovery of a potent and selective inhibitor of cyclin-dependent kinase 4/6. J Med Chem 2005;48:2388–406.
18. Giacinti C, Giordano A. RB and cell cycle progression. Oncogene 2006;25:5220–7.
19. Foster DA, Yellen P, Xu L, Saqcena M. Regulation of G1 cell cycle progression: distinguishing the restriction point from a nutrient-sensing cell growth checkpoint(s). Genes Cancer 2010;1:1124–31.
20. Finn RS, Dering J, Conklin D, Kalous O, Cohen DJ, Desai AJ, et al. PD 0332991, a selective cyclin D kinase 4/6 inhibitor, preferentially inhibits proliferation of luminal estrogen receptor-positive human breast cancer cell lines in vitro. Breast Cancer Res 2009;11:R77.
21. Dean JL, Thangavel C, McClendon AK, Reed CA, Knudsen ES. Therapeutic CDK4/6 inhibition in breast cancer: key mechanisms of response and failure. Oncogene 2010;29:4018–32.

22. Michaud K, Solomon DA, Oermann E, Kim JS, Zhong WZ, Prados MD, et al. Pharmacologic inhibition of cyclin-dependent kinases 4 and 6 arrests the growth of glioblastoma multiforme intracranial xenografts. Cancer Res 2010;70:3228–38.
23. Wiedemeyer WR, Dunn IF, Quayle SN, Zhang J, Chheda MG, Dunn GP, et al. Pattern of retinoblastoma pathway inactivation dictates response to CDK4/6 inhibition in GBM. Proc Natl Acad Sci U S A 2010;107:11501–6.
24. Garnett MJ, Edelman EJ, Heidorn SJ, Greenman CD, Dastur A, Lau KW, et al. Systematic identification of genomic markers of drug sensitivity in cancer cells. Nature 2012;483:570–5.
25. Cuffe S, Moua T, Summerfield R, Roberts H, Jett J, Shepherd FA. Characteristics and outcomes of small cell lung cancer patients diagnosed during two lung cancer computed tomographic screening programs in heavy smokers. J Thorac Oncol 2011;6:818–22.
26. National Lung Screening Trial Research T, Aberle DR, Adams AM, Berg CD, Black WC, Clapp JD, et al. Reduced lung-cancer mortality with low-dose computed tomographic screening. N Engl J Med 2011;365: 395–409.
27. Foote M. The importance of planned dose of chemotherapy on time: do we need to change our clinical practice?Oncologist 1998;3:365–8.
28. Niederst MJ, Sequist LV, Poirier JT, Mermel CH, Lockerman EL, Garcia AR, et al. RB loss in resistant EGFR mutant lung adenocarcinomas that transform to small-cell lung cancer. Nat Commun 2015;6:6377.
29. Shapiro GI, Edwards CD, Kobzik L, Godleski J, Richards W, Sugarbaker DJ, et al. Reciprocal Rb inactivation and p16INK4 expression in primary lung cancers and cell lines. Cancer Res 1995;55:505–9.
30. Matsuura I, Denissova NG, Wang G, He D, Long J, Liu F. Cyclin-dependent kinases regulate the antiproliferative function of Smads. Nature 2004; 430:226–31.
31. Lipinski CA, Lombardo F, Dominy BW, Feeney PJ. Experimental and computational approaches to estimate solubility and permeability in drug discovery and development settings. Adv Drug Deliv Rev 2001;46:3–26.

Molecular Cancer Therapeutics

Preclinical Characterization of G1T28: A Novel CDK4/6 Inhibitor for Reduction of Chemotherapy-Induced Myelosuppression

John E. Bisi, Jessica A. Sorrentino, Patrick J. Roberts, et al.

Updated version	Access the most recent version of this article at: doi:10.1158/1535-7163.MCT-15-0775
Supplementary Material	Access the most recent supplemental material at: http://mct.aacrjournals.org/content/suppl/2016/01/29/1535-7163.MCT-15-0775.DC1.html

Cited articles	This article cites 28 articles, 9 of which you can access for free at: http://mct.aacrjournals.org/content/15/5/783.full.html#ref-list-1

E-mail alerts	Sign up to receive free email-alerts related to this article or journal.
Reprints and Subscriptions	To order reprints of this article or to subscribe to the journal, contact the AACR Publications Department at pubs@aacr.org.
Permissions	To request permission to re-use all or part of this article, contact the AACR Publications Department at permissions@aacr.org.